FI SEVIER

Contents lists available at ScienceDirect

Materials and Design

journal homepage: www.elsevier.com/locate/matdes



Microstructural evolution and interfacial crack corrosion behavior of double-sided laser beam welded 2060/2099 Al-Li alloys T-joints



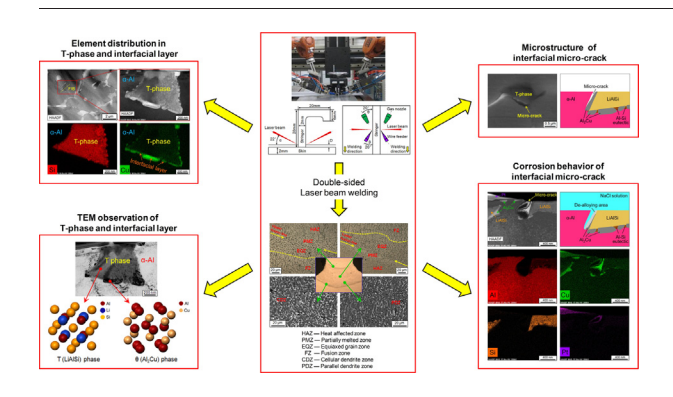
Bing Han ^{a,*}, Yanbin Chen ^{a,*}, Wang Tao ^a, Hao Li ^b, Liqun Li ^a

- ^a State Key Laboratory of Advanced Welding and Joining, Harbin Institute of Technology, Harbin 150001, China
- b National Engineering Research Center of Commercial Aircraft Manufacturing, Commercial Aircraft Corporation of China, Shanghai 200436, China

HIGHLIGHTS

- Interfacial layer between LiAlSi phase and α-Al matrix is composed of alternate Al₂Cu phases and Al-Si eutectics.
- Micro crack is found to be generated along the boundary between interfacial Al₂Cu and α-Al matrix.
- Micro crack can promote Al dissolution in adjacent Al₂Cu phase and α-Al matrix so as to make crack tip propagate.
- No de-alloying is generated in LiAlSi phase even close to de-alloyed Al₂Cu phases.

GRAPHICAL ABSTRACT



ARTICLE INFO

Article history:
Received 16 May 2017
Received in revised form 1 September 2017
Accepted 18 September 2017
Available online 20 September 2017

Keywords:
Aluminum lithium alloys
Double-sided laser beam welding
Microstructural evolution
Interfacial crack
Corrosion behavior

ABSTRACT

2060 and 2099 aluminum lithium (Al-Li) alloys are both the candidate structural materials for Chinese C919 aircraft fuselage panels and their related welding characteristics are greatly different from those of aviation aluminum alloys and need to be studied. Double-sided laser beam welding of 2-mm-thick 2060-T8 and 2099-T83 Al-Li alloys T-joints were successfully performed with 4047 wire. Microstructural evolution and interfacial microcrack corrosion behavior within the weld were investigated. Microstructure analysis results showed that segregation in the weld was featured by the formation of T (LiAlSi), θ (Al₂Cu) and eutectics at grain boundaries. By using focused ion beam (FIB), the interfacial layer between T-phase and α -Al matrix was found to be composed of alternately crystallized θ -phases and Al-Si eutectics. Micro-cracks were observed locating on the boundary between interfacial θ -phase and α -Al matrix. Corrosion test results indicated that the interfacial micro-crack dramatically accelerated the de-alloying in interfacial θ -phase and also the anodic dissolution in adjacent α -Al matrix. However, no corrosion feature was detected in the near surface of T-phase. The continuous selective dissolution of aluminum occurring in front of the micro-crack tip resulted in crack propagation along depth of the boundary between interfacial θ -phase and α -Al matrix.

© 2017 Elsevier Ltd. All rights reserved.

1. Introduction

Due to the remarkable advantages such as relatively low density, high strength-to-weight ratio and elastic modulus, as well as appreciable improvements on toughness and damage tolerance,

^{*} Corresponding authors.

E-mail addresses: dabingzhenniu@163.com (B. Han), taowang81@sina.com (W. Tao).

aluminum lithium (Al-Li) alloys have been considered as desirable potential replacement of traditional 2xxx, 6xxx and 7xxx series aluminum alloys especially in the modern aircraft industry [1–4]. The new third generation 2060 and 2099 Al-Li alloys have been chosen as materials of fuselage panels in the production of the C919 (the first China-made large passenger aircraft). To fulfill further requirement of weight savings on aircrafts, double-sided laser beam welding (LBW) has been successfully utilized on Al-Li fuselage panels manufacturing to partially replace conventional riveting technique [5].

In recent years, published literatures particularly on double-sided LBW Al-Li alloys were mainly focused on weld formation, microstructure, mechanical properties, porosity and cracking susceptibility. Zhang et al. [6] found that welding heat input and laser beam position all showed significant influences on weld penetration and hoop tensile properties. In addition, high welding speed (≥10 m/min) was also favorable for reducing weld porosity. In the early time, Jan et al. [7] studied the influence of the filler elements on the solidification cracking susceptibility in CO₂ laser welding of 2195 Al-Li alloy butt joint using different filler wires such as Al-Si, Al-Mg and Al-Cu alloy wires, and finally the Al-Si wire was found to be more effective on reducing the susceptibility of solidification cracking. In double-sided LBW Al-Li alloys, however, relative simulation results of Zain-ul-abdein et al. [8] comparatively studied weld residual stress distribution characteristics between conventional butt joint and particular T-joint. More serious post-weld residual tensile stress within T-joint was detected. Tian et al. [9] also proposed that hot cracking still could not be effectively restrained in double-sided LBW 2196/2198 Al-Li alloys T-joint even by using AlSi12 wire. Hot cracks in double-sided LBW 2060/2099 Al-Li alloys T-joint using AlSi12 wire were also observed in our previous studies [10,11]. Enz et al. [5] investigated the relationship between Si-content and mechanical properties in the weld zone of T-joint, and suggested that mechanical property fluctuation and even defect formation were all affected by the inhomogeneous distribution of Si element. In addition, limited studies on precipitated phases in LBW 2060 Al-Li alloy butt joint had been reported. Zhang et al. [12] studied precipitate types in LBW 2060 Al-Li alloy weld using AlSi12 wire, and found that the LiAlSi, Al₂Cu phases and a small quantity of Mg₂Si phase were located at the dendritic and grain boundaries to reduce the precipitation ability in the interior of grains. In particular, Zhang et al. [13] detected an icosahedral quasicrystalline phase of Al₆CuLi₃ in LBW 2060 Al-Li alloy weld when using an Al-Mg 5087 wire. Ning et al. [14] also comparatively studied microstructural inhomogeneity in the welds of autogenous (ALW) and nonautogenous laser welding (NLW) by microhardness tests and found that different from significant microhardness inhomogeneity both in the width and thickness directions in the NLW weld, only obvious microhardness differences in the width direction were presented in the ALW weld.

Compared with the studies of LBW Al-Li alloys butt joints, different precipitation characteristics could still be obtained in double-sided LBW Al-Li alloys T-joints due to the differences on welding parameters, thermal cycle, pool flow field and residual stress level in welding process. To the best of our knowledge, however, no more detailed investigation particularly on precipitated phases in the weld of double-sided LBW Al-Li alloys T-joint has been published till now. The purpose of the present study is to further investigate precipitation and unpublished interfacial micro-crack characteristics in double-sided LBW T-joints of 2060/2099 Al-Li alloys.

2. Experimental procedures

The new generation of 2060-T8 and 2099-T83 Al-Li alloys with a similar thickness of 2 mm were chosen for the skin and stringer components, respectively. Two ER 4047 (AlSi12) filler wires with the uniform diameter of 1.2 mm were used in welding process. The chemical compositions of the base metals (BMs) and the filler wire are given in Table 1. In order to eliminate weld pores, the surfaces of the skin and stringer

Table 1Chemical compositions of the base metals and the filler wire.

Alloy	Element (wt%)								
	Cu	Si	Li	Zn	Mg	Mn	Zr	Ag	Al
2060 2099 4047	3.9 2.52 <0.01	0.02 - 11.52	0.8 1.87 -	0.32 1.19 0.001	0.7 0.497 0.01	0.29 0.309 0.01	0.1 0.082 -	0.34 - -	Bal. Bal. Bal.

materials were prepared by chemical cleaning followed by drying in a drying furnace before welding.

T-joints, parallel to the skin's rolling direction, were welded using a welding system composed of two 10 kW fiber lasers (YLS-10000, IPG Photonics Corp., Germany), two 6-axis industrial robots (KR-16W, KUKA Robot Group, Germany) and two wire feeders (KD-4010, Fronius International GmbH, Austria), as shown in Fig. 1a. The fiber lasers with the emission wavelength of 1.07 µm can deliver in continuous wave (CW) mode. The laser beam passed through a focusing mirror with 192 mm focus length and was finally focused on a spot of 0.26 mm in diameter. The primary welding parameters, previously optimized, were laser power of 3.0 kW, welding velocity of 10.0 m/min, wire feeding rate of 4.3 m/min, wire extension of 8 mm and shielding gas flow rate of 15 L/min. The above welding parameters were derived from numerous experimental results [11]. The welding method and joint configuration used in this study are illustrated in Fig. 1b. The two fiber laser beams should be focused symmetrically onto two opposite sides of the stringer with uniform included angle of 22°. The filler wire and shielding gas were delivered on the same plane as the laser beam and held at an angle of 20° to the stringer in leading and trailing directions, respectively. No heat treatment was performed on the welded T-joints post welding.

After welding, the cross sections were made in a direction perpendicular to the welding direction. Microstructural evolutions were performed on the cross section of the T-joint by optical microscopy (OM, OLYMPUS-GX71), scanning electron microscopy (SEM, FEI Quanta-

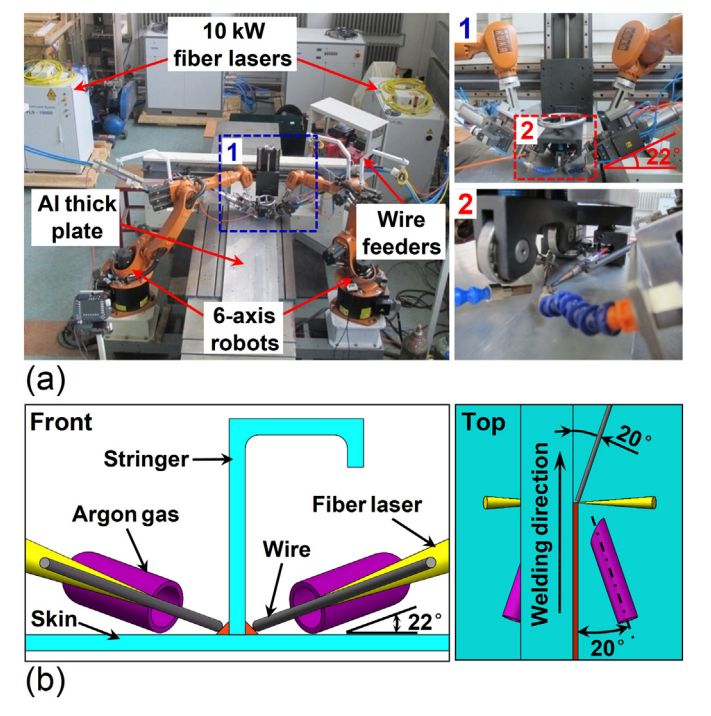


Fig. 1. (a) Laser welding facility and (b) schematic diagrams of the T-joint configuration.

Download English Version:

https://daneshyari.com/en/article/5023134

Download Persian Version:

https://daneshyari.com/article/5023134

<u>Daneshyari.com</u>